Molecular Dynamics Study of Surfactant Monolayers Adsorbed at the Oil/Water and Air/Water Interfaces

Jnanojjal Chanda and Sanjoy Bandyopadhyay*

Molecular Modeling Laboratory, Department of Chemistry, Indian Institute of Technology, Kharagpur, 721302, India

Received: May 25, 2006; In Final Form: August 16, 2006

Atomistic molecular dynamics (MD) simulations have been carried out to investigate the physical properties of monolayers of monododecyl diethylene glycol ($C_{12}E_2$) surfactants adsorbed at the oil/water and air/water interfaces. The study shows that the surfactant molecules exhibit more extended conformations with a consequent increase of the thickness of the monolayer in the presence of the oil medium. It is noticed that the hydrocarbon tails of the surfactants are more vertically oriented at the oil/water interface. Interestingly, we notice that the presence of the oil medium has a strong influence in restricting both the translational and reorientational motions of the water molecules present in the hydration layer close to the surfactant headgroups.

1. Introduction

A microscopic understanding of the properties of surfactant assemblies organized at an interface is not only of interest in basic research in surfactant science, but is also of great importance in various industrial processes, such as detergency, separation, purification, food processing, lubrication, and so forth.[1−3]

This study is focused on the surfactant $C_{12}E_2$, which is a member of an important class of nonionic surfactants, known as the C_mE_n family. These are monoalkyl ethers of the form $C_mH_{2m+1}(OC_2H_4)_nOH$, with a long headgroup consisting of a hydroxy (OH) group followed by a variable number of polar oxyethylene (OC_2H_4 or E) groups, and a nonpolar C_mH_{2m+1} hydrocarbon tail, also of variable length. These are one of the most important nonionic surfactants in commercial use.[1]

Although significant effort has been made to study the surfactant aggregates at interfaces, a molecular level understanding of the properties of such aggregates is still lacking. Pulsed-field gradient NMR experiments have been used to measure the diffusion coefficients of individual components in a water−AOT−decane microemulsion at different temperatures.[4] Richmond and co-workers[5−7] have studied the conformational ordering of surfactants as well as the properties of interfacial water molecules for monolayers adsorbed at the air/water and carbon tetrachloride (CCl_4)/water interfaces at different surface coverages. The collective properties and dynamics of different surfactants (ionic and nonionic) adsorbed at the nitrobenzene/water interface have been studied by using time-resolved quasielastic laser scattering experiments.[8] Earlier, fluorescence[9] and resonance Raman[10] spectroscopic experiments have also been used on different surfactant films adsorbed at liquid/liquid interfaces. Surface tension and ellipsometric measurements are employed by Linse and co-workers[11] to study nonionic surfactants at vapor/liquid and solid/liquid interfaces. Thomas and co-workers[12−17] have successfully employed neutron reflection techniques with isotopic substitutions to study the properties of different types of surfactant films adsorbed at air/liquid, liquid/liquid, and solid/liquid interfaces. These studies provide microscopic information on various properties of adsorbed films, such as the density profiles of different components, thickness of the films, as well as the orientation of the surfactant molecules at the interfaces.

Several computer simulation studies have been attempted in the recent past to study the microscopic properties of surfactant assemblies at different interfaces.[18−29] In an early MD simulation study, Tarek et al.[18] reported the properties of a cationic surfactant cetyltrimethylammonium bromide (CTAB) adsorbed at the air/water interface at different concentrations. Their results were in good agreement with experimental data. Wijmans and Linse[19] have reported Monte Carlo studies on the self-assembly of nonionic surfactants at a hydrophilic surface. Kuhn and Rehage[20−22] have studied in detail the orientation and dynamic properties of monododecyl pentaethylene glycol ($C_{12}E_5$) monolayers adsorbed at the air/water and oil/water interfaces. Recently, Rossky and co-workers[24] have shown that water penetrates less into a fluorocarbon surfactant monolayer as compared to that for hydrocarbon surfactants at the CO_2/water interface. Smit and co-workers[25,26] have recently used dissipative particle dynamics simulations to study the effect of surfactant structure on the bending moduli of the adsorbed monolayers. We have recently studied in great detail the microscopic properties of both ionic as well as nonionic surfactant monolayers adsorbed at the air/water interface.[27−29] Our studies revealed that the interfacial water molecules have a strong influence on the orientational and other properties of the surfactant molecules.

In this work, we report the microscopic properties of monolayers of monododecyl diethylene glycol, $C_{12}E_2$, adsorbed at the oil/water interface using atomistic MD simulation methods. We have used decane to model the oil medium in this study. We have compared the results with another simulation of $C_{12}E_2$ monolayers adsorbed at the air/water interface with a surface coverage corresponding to that at the critical micelle concentration or cmc. The effects of the presence of the oil medium on the structure and dynamics of the surfactants as well as that on the hydration layer water molecules have been investigated in detail. To the best of our knowledge, this is the

* To whom correspondence should be addressed. E-mail: sanjoy@chem.iitkgp.ernet.in. Phone: 91-3222-283344. Fax: 91-3222-255303.

10.1021/jp063205o CCC: $33.50
Published on Web 10/25/2006

first simulation study where the influence of an oil medium on the dynamical properties of water in the aqueous layer near the surfactant headgroups has been studied. The rest of the article is organized as follows. In the next section, we discuss the setup of the two simulation systems and a brief description of the methodologies employed. This is followed by the results obtained from our investigations and their interpretation. In the last section, we summarize the important findings obtained from our study.

2. System Setup and Simulation Details

Two different simulations have been carried out. In the first simulation, monolayers of $C_{12}E_2$ surfactants adsorbed at the air/water interface have been studied. The initial configuration of this system was set up by arranging a uniform monolayer of 64 surfactants with the hydroxy (OH) group on an appropriate 8 $\times$ 8 square lattice in the *xy* plane with the hydrocarbon chains extending perpendicular to this plane with fully extended conformations. The lattice constants were chosen to give the surface area per molecule of 34 Å^2, corresponding to the experimentally observed value for adsorption at the air/water interface at the cmc.[30] Then two such Langmuir-type monolayers were placed, with their OH groups solvated in the *xy* plane of a roughly 30 Å thick slab of water. The overall system contained 128 surfactants and 2127 water molecules. The dimension of the simulation cell in the *x* and *y* directions was 46 Å, while the *z* dimension was kept at 100 Å.[27] A short MD run of 10 ps was first performed at 1000 K, keeping the surfactant headgroups and the water molecules fixed, to randomize the hydrocarbon chain conformations of the surfactants. Then the headgroups and the water molecules were unfrozen and the temperature of the system was lowered to 10 K. The temperature was then slowly increased to room temperature (298 K) over next 50 ps. The resulting configuration was then equilibriated at constant volume and at room temperature for about 1 ns. This was followed by a production run of another 2 ns duration. The further details of the air/water simulation system can be found elsewhere.[27]

In the second simulation, monolayers of $C_{12}E_2$ surfactants adsorbed at the oil/water interface have been studied. The configuration with randomized hydrocarbon tails of the surfactants as obtained at the end of the first 10 ps of the air/water simulation at 1000 K was taken to set up the initial configuration of the oil/water system. Then two 20 Å thick slabs of liquid decane were placed on the two sides of the monolayers in the *z* direction. The overall system contained 128 surfactants, 2127 water molecules, and 256 decane molecules with 124 Å initial dimension of the cell in the *z* direction. At first, the system was equilibrated in a constant normal pressure, constant area ensemble for a short duration of about 100 ps at 298 K. During this period, the dimension of the simulation cell in the plane of the interface (i.e., *xy* plane) was kept fixed to that used for the air/water simulation, while the dimension in the direction normal to the interface (i.e., along *z*) was allowed to fluctuate at constant pressure. At the end of this short duration, the dimension of the simulation cell along the *z* direction attained a steady value of 115.8 Å. The equilibration was further continued for about 2 ns at constant temperature (298 K) and volume (NVT). This was followed by a NVT production run of over 4.5 ns duration. The MD trajectories were stored for both the air/water and the oil/water systems for subsequent analysis.

All the simulations reported in this work utilized the Nosé−Hoover chain thermostat extended system method[31] as implemented in the PINY-MD simulation code.[32] A recently developed reversible multiple time step algorithm, RESPA,[31] has been employed to integrate the equation of motions. This was achieved by using a three-stage force decomposition into intramolecular forces (torsion/bend-bond), short-range nonbonded forces, and long-range nonbonded forces. Electrostatic interactions were calculated by using the particle mesh Ewald (PME) method.[33] The PME and RESPA were combined following the method suggested by Procacci et al.[34,35] The minimum image convention[36] was employed to calculate the Lennard-Jones interactions and the real-space part of the Ewald sum, using a spherical truncation of 7 and 10 Å, respectively, for the short- and the long-range parts of the RESPA decomposition. A longest time step of 4 fs was used to integrate the nonbonded interactions between 7 and 10 Å, while a 2 fs time step was used to integrate the nonbonded interactions within 7 Å. The intramolecular torsional degrees of freedom were integrated with a time step of 1 fs, and the bond stretching and bending interactions were integrated with a 0.5 fs time step. "SHAKE" and "RATTLE" methods[31] were implemented to constrain all bonds involving hydrogen atoms to their equilibrium values.

The intermolecular potential model was based on pairwise additive site−site electrostatic and Lennard-Jones contributions. The rigid three-site SPC/E model[37] was employed for water. The CH_3 and CH_2 groups of the surfactants were treated as united atoms (i.e., these groups were represented by single interaction sites). The potential parameters for the alkane chain groups were taken from the work of Martin and Siepmann,[38] while the oxyethylene groups were modeled by using the OPLS parameters.[39,40] The surfactant chains were made flexible by including bond stretching, bending, and torsion interactions.

3. Results and Discussion

3.1. Structural Properties. Figure 1 shows the configurations of the simulation system (cross-sectional view normal to the plane of the interface) at the beginning and at the end of the oil/water simulation. The most notable feature of the figure is the development of significant roughness during the simulation around the headgroups as well as the tail region of the surfactants at the interface. The figure also indicates sufficient mixing between different components of the system. The microscopic details of the structural properties of adsorbed monolayers can be obtained from various distribution functions. In Figure 2, we display the average number density profiles (NDP) of different components of the surfactant molecules as obtained from the oil/water simulation and measured from the center of the simulation cell and in the direction normal to the plane of the interface (i.e., along *z*). The different components of the surfactant molecules for which the density profiles are calculated include the terminal hydroxy group (OH), the oxyethylene groups (E), and the hydrocarbon chain atoms (C). The distributions of water and decane molecules are also computed and included in the plot. The essential features of the distributions corroborate well with the general picture of surfactants adsorbed at an interface.[18,23,27−29,41] The surfactant headgroups are mostly hydrated, whereas the hydrocarbon tails are excluded from the aqueous layer. Only a small fraction of water penetrates into the tail region of the surfactants. Interestingly, significant overlapping between the decane molecules and the hydrocarbon tails of the surfactants is also observed. A small fraction of the decane molecules is also in close contact with the oxyethylene headgroups of the surfactants. It may be noted that the density profiles of the two monolayers are essentially symmetric, indicating a well-equilibrated system with similar overall

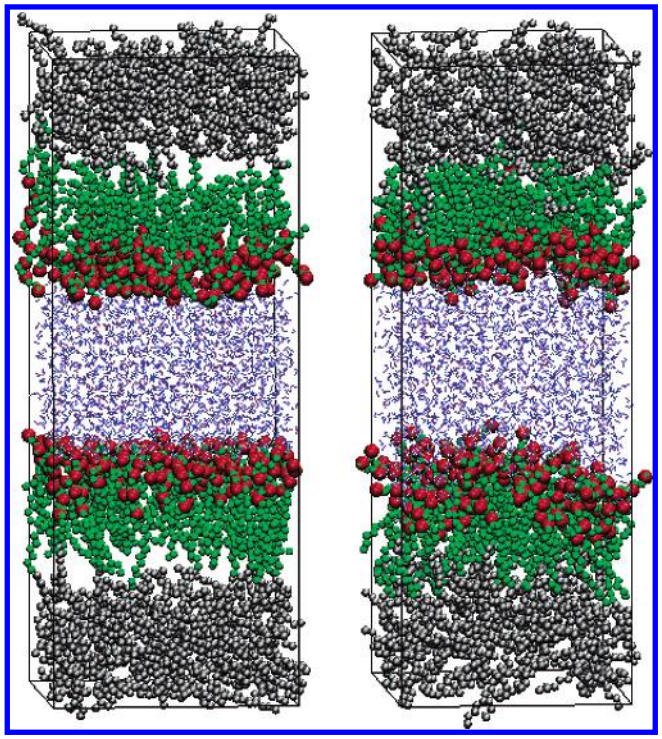

Figure 1. Snapshots of the configuration of the system near the beginning (left) and at the end (right) of the oil/water simulation. The oxygen atoms, methyl (CH_3), and methylene (CH_2) groups of the surfactants and decane molecules are drawn as spheres, while the water molecules are drawn as sticks. The atom coloring scheme is, O (surfactant), red; CH_3/CH_2 (surfactant), green; decane, gray; and O (water), blue.

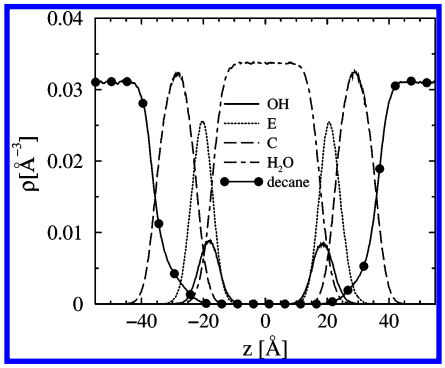

Figure 2. Number density profiles of the hydroxy group (OH), oxyethylene groups (E), hydrocarbon chain atoms (C), water, and decane molecules, measured with respect to the center of the simulation cell and in the direction normal to the plane of the interface (i.e., along *z*) as obtained from the oil/water simulation system.

structure of the two monolayers. The presence of a 20−25 Å thick slab of bulk water and decane separating the two surfactant monolayers indicates that they are independent and have practically no influence on each other.

The presence of decane molecules may influence the thickness of the adsorbed surfactant monolayers as compared to that at the air/water interface.[27] We have measured the thickness of the adsorbed monolayers from the simulated trajectory of the oil/water system. The time evolution of the thickness of the oxyethylene (E) headgroup part (d_h), the dodecyl hydrocarbon tail (d_t), as well as the total thickness (d_s) of the layers are shown in Figure 3. The thickness d_h at a particular time step is defined as the magnitude of the separation between the maximum and minimum coordinates of the hydrogen atom of the terminal OH group and the second oxyethylene group oxygen atom along

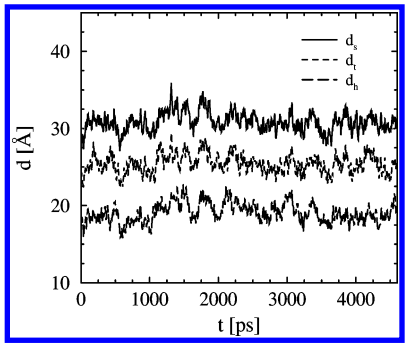

Figure 3. Time evolution of the thickness of the monolayer during the last 4.5 ns of the oil/water simulation. The thickness of the whole surfactant chain (d_s) is drawn as a solid line, while those of the oxyethylene headgroup (d_h) and the hydrocarbon tail (d_t) are drawn as broken lines. The calculation is done by averaging over both monolayers.

TABLE 1: The Oxyethylene Group Thickness (d_h), Dodecyl Chain Thickness (d_t), and the Total Thickness (d_s) of $C_{12}E_2$ Monolayers Adsorbed at the Oil/Water and the Air/Water Interfaces

quantity(Å)	oil/water	air/water
d_h	19.1 ± 0.8	15.0 ± 0.4
d_t	25.4 ± 1.0	19.5 ± 0.3
d_s	30.8 ± 1.0	25.0 ± 0.4

the *z* axis. Similarly, d_t is defined as the separation between the maximum and minimum *z*-coordinates of the first methylene group and the terminal methyl group of the dodecyl tail, while d_s is the corresponding separation for the entire surfactant molecule. The calculations are carried out by averaging over the surfactants in both the monolayers. The roughness of the adsorbed monolayers is clearly apparent from the sharp oscillations in the plots. The average thickness values as obtained from our calculations are listed in Table 1. For comparison, we have also listed the corresponding values for the adsorbed surfactant films at the air/water interface as reported earlier.[27] It is clear that the thickness of different components of the surfactant molecules and the total thickness of the monolayer at the oil/water interface are approximately 25−30% higher than that at the air/water interface. This is primarily due to strong hydrophobic interaction between the decane molecules and the hydrocarbon tails of the surfactants, resulting in mixing between the oil medium and the surfactants. We have observed that in the presence of decane, on average 81% of the C−C bonds of the dodecyl chains of the surfactants are in the trans form, compared to about 75% in the absence of decane. Thus, the presence of the oil medium results in extended conformations of the hydrocarbon tails of the surfactants with a reduction of chain defects. This leads to an expansion of the monolayer with a consequent increase of its thickness in the presence of the oil medium. Besides, it can be seen that the sum of the thicknesses of the two constituent parts of the surfactant molecules (d_h and d_t) is greater than the total thickness (d_s) of the monolayer. This indicates that an extensive mixing of the head and the tail parts of the surfactant molecules occurs at the oil/water interface, which is similar to that observed for adsorbed monolayers at the air/water interface.[27−29] Such mixing is in accordance with the density distributions, as shown in Figure 2.

We have calculated the interfacial surface tension (γ) for both the air/water and the oil/water systems, which is related to the diagonal components of the pressure tensor as[42,43]

$$\gamma = \frac{1}{2}L_z\left[P_{zz} - \frac{1}{2}(P_{xx} + P_{yy})\right] \quad (1)$$

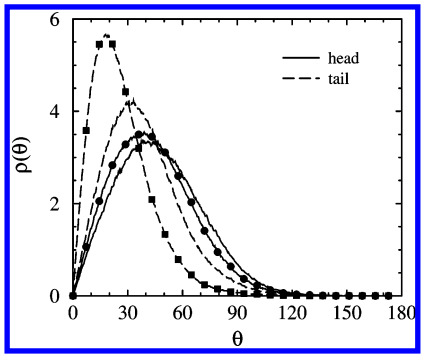

Figure 4. Distribution of the tilt angle, θ (in degrees), of the oxyethylene headgroups and the hydrocarbon tails of the surfactants with respect to the normal to the interface (i.e., with the *z* axis) for both the oil/water (with symbols) and the air/water (without symbols) simulation systems.

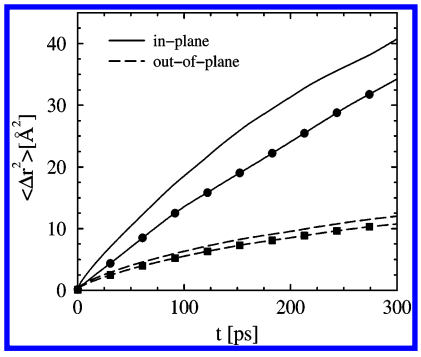

Figure 5. Time evolution of the in-plane (i.e., in *xy* plane) and the out-of-plane (i.e., along *z*) mean square displacements of the center of mass of the surfactant molecules adsorbed at the oil/water (with symbols) and the air/water (without symbols) interfaces.

where L_z and P_{zz} denote the dimension of the simulation cell and the component of the pressure tensor in the direction normal to the interface (i.e., along *z*), respectively, and P_{xx} and P_{yy} are the tangential components of the pressure tensor. The pressure tensors of the systems have been calculated along the simulated trajectories by averaging over the two equivalent interfaces in each of the systems. The calculated average surface tension values for the air/water and the oil/water systems are found to be 36.3($\pm$0.1) and 2.0($\pm$0.2) mN m^{-1}, respectively. Small error bars associated with the estimated surface tension values indicate that both the systems are in well-equilibrated states. The experimental value of surface tension for the $C_{12}E_2$ monolayer adsorbed at the air/water interface at cmc is $\sim$32 mN m^{-1}.[30] Thus the simulated result for the air/water system is in good agreement with experimental data. This implies that the force field and the potential parameters employed in this study are accurate enough for studying such interfacial systems. As expected, the surface tension decreases drastically in the presence of the oil medium. This is consistent with earlier simulation studies on different surfactant systems.[44]

3.2. Orientation of Surfactants. It would be interesting to investigate the orientation of the surfactant molecules at the interface in the presence of oil. This is studied by measuring the angle between the oxyethylene head vectors or the dodecyl hydrocarbon tail vectors of the surfactants and the normal to the plane of the interface (i.e., with the *z* axis). The head vector is defined as the vector connecting the hydroxy group and the oxygen atom of the second oxyethylene group, while the vector that connects the first methylene and the terminal methyl groups of the surfactant dodecyl chain is defined as the tail vector. The probability distributions, $\rho(\theta)$, of the tilt angles (θ) of the head and tail vectors of the surfactants with respect to the normal to the plane of the interface (*z*) for the oil/water system are displayed in Figure 4. The distributions are calculated by averaging over both the monolayers. For comparison, we have also included in the figure the corresponding distributions for $C_{12}E_2$ monolayers adsorbed at the air/water interface, as reported earlier.[27] The figure shows that the oxyethylene headgroups of the surfactants are tilted more than the dodecyl tails from the normal to the interface for both the oil/water and the air/water systems. It is clear from the figure that the orientation of the headgroups at the oil/water interface resembles closely that at the air/water interface, while a significant difference in the orientation of the surfactant tails is noticed. The average tilt angles (θ_{avg}) for the head and the tail vectors have been found to be 43.9° and 27.1° at the oil/water interface, as compared to 48.4° and 38.5°, respectively, at the air/water interface. Thus, while θ_{avg} is decreased by less than 10% for the oxyethylene head vectors, it is decreased by $\sim$30% for the dedecyl tail vectors. This is an interesting observation and is in agreement with the extended conformation of the dodecyl tails in the presence of oil. Thus the favorable interaction between the decane molecules in the oil medium and the surfactant tails not only allows the latter to attain extended conformations but also to orient them almost parallel to the *z* axis or normal to the interface. This result is in agreement with neutron reflection studies by Thomas and co-workers,[15] where they showed that the orientation of surfactant chains becomes almost vertical in the presence of an oil medium.

3.3. Dynamics at the Interface. The microscopic dynamics of different components of a surfactant film adsorbed at an interface plays an important role in determining the properties of the film. In this section the dynamics of the surfactants and the water molecules around them are discussed.

3.3.1. Surfactant Dynamics. The translational motion of the surfactant molecules is studied by measuring the time dependence of their center of mass mean square displacements (MSD) for both the oil/water and the air/water simulation systems. As the adsorbed monolayers are anisotropic in the direction normal to the plane of the interface, we have separately calculated the MSDs of the surfactants in the plane of the interface (i.e., in the *xy* plane) and in the out-of-plane direction (i.e., along *z*). The results are displayed in Figure 5. It is clear from the figure that irrespective of the type of interface (oil/water or air/water), the surfactant molecules exhibit higher mobility in the plane of the interface. Such relatively higher in-plane mobility of surfactant monolayers adsorbed at an interface has been reported earlier for both ionic and nonionic surfactants.[28,29] This primarily arises from the lateral rattling motion of the surfactant molecules, which dominates the time scale over which the calculations are carried out. The out-of-plane protrusion motion of the surfactants is more restricted at both the oil/water and the air/water interfaces. Such restricted dynamics of surfactants at an interface is an indication of anomalous sublinear diffusion in heterogeneous anisotropic or confined systems.[45,46] To study the extent of such anomaly, the MSD values are fitted to a law

$$\langle \Delta r^2 \rangle \approx t^{\alpha} \qquad (2)$$

where the exponent α is expected to be smaller than 1 if the diffusion is sublinear. The estimated values of α for the in-plane and the out-of-plane motions of the surfactants are found to be 0.58 and 0.38 at the oil/water interface, as compared to 0.64 and 0.41, respectively, at the air/water interface. Such small α values demonstrate the existence of significant sublinear diffusion behavior of surfactants adsorbed at interfaces. Such an anomaly is more prominent for the out-of-plane mobility of

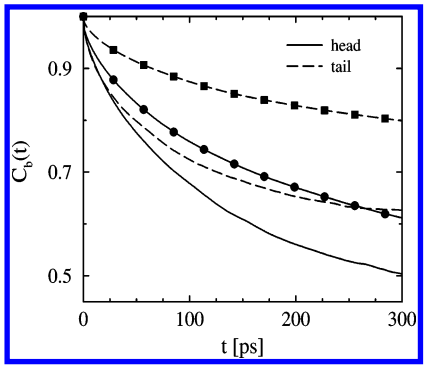

Figure 6. Reorientational time correlation functions, $C_b(t)$, for the oxyethylene head vectors and the hydrocarbon tail vectors of the surfactant molecules adsorbed at the oil/water (with symbols) and the air/water (without symbols) interfaces.

the surfactants. Interestingly, there is a noticeable decrease in both the in-plane and the out-of-plane mobility of the surfactant molecules at the oil/water interface. This is an important observation, which suggests that the surfactant films are more rigid in the presence of an oil medium.

It would be interesting to investigate the effect of the presence of the oil medium on the internal dynamics of the surfactant molecules or the fluidity of the monolayer interior. This is done by measuring the reorientational dynamics of the oxyethylene head and the dodecyl hydrocarbon tail vectors (as defined earlier) of the individual surfactants of both the systems. The reorientational motion has been analyzed by measuring the time correlation function (TCF), $C_b(t)$, defined as

$$C_b(t) = \frac{\langle \hat{b}_i(t+\tau) \cdot \hat{b}_i(\tau) \rangle}{\langle \hat{b}_i(\tau) \cdot \hat{b}_i(\tau) \rangle} \tag{3}$$

where $\hat{b}_i(t)$ represents the unit vector corresponding to the head or tail of the ith surfactant molecule at time t, and the angular brackets denote averaging over the surfactant molecules and over initial times τ. The variation of $C_b(t)$ against time has been displayed in Figure 6 for both simulation systems. At first, it can be seen that the reorientation of both the head and the tail parts of the surfactant molecules is slower in the presence of the oil medium. This is in accordance with the differences between the translational mobility of the surfactants with and without the presence of the oil (Figure 5). Therefore, Figure 6 further confirms that the rigidity of the surfactant monolayer increases in the presence of oil. Due to penetration of the decane molecules into the hydrocarbon tail region of the monolayer, the rotational motion of the tail group is severely restricted. The influence of the oil component is so prominent that the reorientation of the oxyethylene headgroups of the surfactants is also affected quite significantly.

3.3.2. Water Dynamics. The dynamics of water present near the hydrophilic headgroups of surfactants plays a crucial role in determining the behavior of surfactant assemblies, both in solutions and at interfaces. Water dynamics at the surface of organized molecular assemblies in solutions, such as micelles,[47−49] is well studied. However, only a few studies are reported on the dynamics of water at the interface of adsorbed surfactant films.[28,29] In this section, we study the translational and reorientational motions of water near the interface.

We have calculated the mean square displacements of water molecules that are in close proximity to the surfactant headgroups at the interface. To be specific, we have performed the calculations for those water molecules which reside within 4 Å from the hydroxy group oxygen atoms of the surfactant

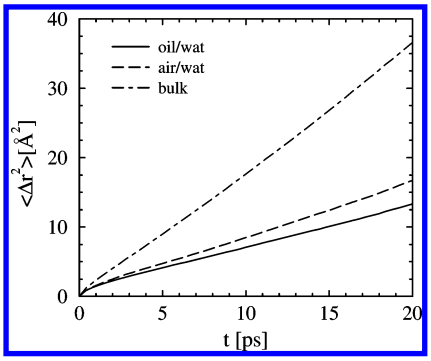

Figure 7. Time evolution of the mean square displacements of water molecules present in the hydration layer of the surfactant headgroups for both the oil/water and the air/water simulation systems. Only those water molecules which reside within 4 Å from the hydroxy group oxygen atoms of the surfactant headgroups are considered. The MSD data for pure bulk SPC/E water are also displayed for comparison.

headgroups. This distance essentially corresponds to the first hydration layer with respect to the hydroxy group oxygen atoms of the surfactants.[27,29] The distances are measured with respect to both the monolayers by tagging the water molecules at different time origins. The results are displayed in Figure 7 for both the oil/water and the air/water systems. For comparison, we have also shown the MSD of pure bulk water, as obtained from a MD simulation of pure SPC/E water under identical conditions. It is evident from the figure that the translational mobility of the hydration layer water in both the simulation systems is restricted as compared to pure bulk water. Such restricted motion of water present in the hydration layer of organized molecular assemblies, such as micelles, and surfactant aggregates at interfaces has been studied recently.[28,29,47−49] This primarily arises because of the strong interaction between the hydrophilic headgroups of the surfactants and the surrounding water molecules.[28,29] Interestingly, we find a small but noticeable decrease in the mobility of the hydration layer water in the presence of the oil medium. This agrees well with the decrease in surfactant mobility and a consequent increase of the rigidity of the surfactant monolayer in the presence of oil. Thus the result indicates that the dynamics of the surfactants and the hydration layer water molecules are strongly coupled.

In a similar fashion, we have looked into the rotational dynamics of the hydration layer water molecules of the two monolayer systems. This is done by measuring the reorientational dynamics of the electrical dipole of water $\vec{\mu}$, defined as the vector connecting the oxygen atom of a water molecule, to the center of the line joining the two hydrogen atoms. The time evolution of $\vec{\mu}$ can be estimated by measuring the dipole−dipole time correlation function (TCF), defined as

$$C_\mu(t) = \frac{\langle \hat{\mu}_i(t+\tau) \cdot \hat{\mu}_i(\tau) \rangle}{\langle \hat{\mu}_i(\tau) \cdot \hat{\mu}_i(\tau) \rangle} \tag{4}$$

where $\hat{\mu}_i(t)$ is the unit dipole moment vector of the ith water molecule at a time t, and the angular brackets denote averaging over the tagged water molecules present in the hydration layer at different initial times τ. Again, we restrict ourselves to the reorientational motion of only those water molecules which are in the first hydration shell (i.e., within 4 Å) of the hydroxy group oxygen atoms of the surfactant headgroups. The results are displayed in Figure 8. The correlation function for pure bulk water is also shown for comparison. As observed for the translational dynamics (Figure 7), the reorientational motion of water molecules present in the hydration layer is restricted too

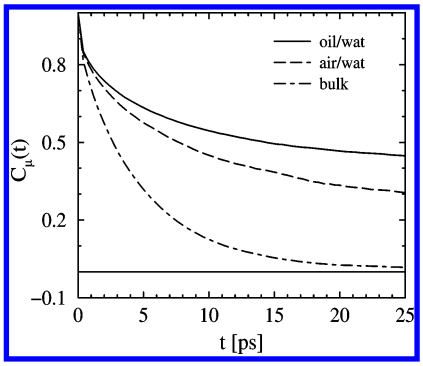

Figure 8. Reorientational time correlation function (TCF) of the water dipoles, $C_\mu(t)$, for the water molecules present in the hydration layer of the surfactant headgroups for both the oil/water and the air/water simulation systems. The definition of the hydration layer is the same as in Figure 7. The corresponding correlation function for pure bulk SPC/E water is also displayed for comparison.

TABLE 2: Multiexponential Fitting Parameters for the Dipolar Time Correlation Functions of the Hydration Layer Water Molecules for the Oil/Water and the Air/Water Simulation Systems[a]

system	time constant (ps)	amplitude (%)	$\langle\tau_\mu\rangle$ (ps)
oil/water	0.26	15.3	68.86
	5.06	30.3	
	123.69	54.4	
air/water	0.26	15.4	27.46
	5.24	36.7	
	53.23	47.9	
bulk water	0.22	13.8	4.73
	4.68	80.6	
	16.63	5.6	

[a] $\langle\tau_\mu\rangle$ is the average time constant. Corresponding parameters for pure bulk SPC/E water are also listed for comparison.

for both simulation systems, as compared to that for pure bulk water. It may be noted from the figure that the relaxation of $C_\mu(t)$ for the interfacial water molceules takes a rather long time to approach zero with respect to pure bulk water. Such slow decay arises due to the presence of a fraction of water molecules which are strongly bound to the oxyethylene headgroups by hydrogen bonds,[27] and thus remain trapped in the monolayer for longer durations. We observed similar restricted rotation of water at the interface of other surfactant monolayers at the air/water interface.[28,29] Here, we notice that the relaxation of the correlation function is further slowed in the presence of oil. One can obtain an estimation of the time scales associated with the reorientational motion of the water molecules from the dipolar correlation functions. As all the curves exhibit slower decay at long times, they cannot be described by a single-exponential law. We have fitted the decay curves to multi-exponentials to extract the time constants associated with the rotational motions.[28,29] We have used a sum of three exponentials, and the parameters for best fit along with the amplitude-weighted average time constants ($\langle\tau_\mu\rangle$) are listed in Table 2. Broadly, three different rotational time scales have been identified for both monolayer systems, starting from ultrafast to slow components. Such different time scales arise due to the presence of different types of water molecules in the hydration layer, ranging from bound to free water molecules. The initial ultrafast component (~250 fs) arises from the high-frequency librational (hindered rotation) motion of the free water molecules. Damped rotational motions of these water molecules are likely to contribute to the relaxation with time constant ~5 ps. The slow component (50−120 ps) observed for the air/water and the oil/water systems arises from those interfacial water molecules which are bound to the surfactant headgroups, as mentioned earlier. The value of the long time component provides a direct measure of the degree of restriction of the rotational motion of these bound water molecules. It can be seen from Table 2 that the long time component for the oil/water system is more than twice as large as the corresponding component for the air/water system. It is clear that the rotational motion being a faster process has been influenced more than the translational motion in the presence of the oil medium.

4. Conclusions

Let us first summarize the main results of this work. We have carried out atomistic MD simulations to study the properties of self-assembled monolayers of the nonionic surfactant $C_{12}E_2$ adsorbed at an oil/water interface. We have used decane as the oil medium. The simulation is performed at constant volume and at a temperature of 298 K. Various structural and dynamical properties of the components of the system have been investigated in microscopic detail. To understand the effects of the oil medium on surfactant properties, the results are compared with that obtained from another simulation of $C_{12}E_2$ monolayers adsorbed at the air/water interface under identical conditions, and with available experimental data. The simulations indicate the presence of significant roughness at the interfacial regions, near both the aqueous and the oil mediums. Significant overlapping between the decane molecules and the hydrocarbon tails of the surfactants is observed. We have noticed that a strong hydrophobic interaction between the decane molecules in the oil medium and the hydrocarbon tails of the surfactants leads to more extended conformations of the latter. As a result, the thickness of the monolayer at the oil/water interface is larger than that at the air/water interface. Importantly, it is also noticed that in the presence of oil the surfactant tails are more vertically oriented, which is in agreement with experimental results.[15]

The dynamics of the surfactants and the water molecules present in the hydration layer are also investigated in detail. We have observed significant anomaly in the diffusion behavior of the surfactants in both systems. Interestingly, we found that both translational and rotational mobility of the surfactants are slowed in the presence of oil. This indicates an increase of rigidity of the surfactant monolayer due to the presence of the oil component. The translational and reorientational motions of the hydration layer water molecules are found to be restricted in both the oil/water and the air/water interfaces. However, more importantly, it is observed that the water mobility is decreased in the presence of the oil medium. Rotational motion of water being faster has been found to be influenced more significantly than the translational motion.

It would be interesting to investigate whether the presence of an oil medium affects the properties of adsorbed films of other classes of surfactants, such as ionic surfactants. That will enable us to obtain a general understanding of surfactant properties at the oil/water interface. Work is in progress in this direction in our laboratory.

Acknowledgment. This work was supported in part by generous grants from the Council of Scientific and Industrial Research (CSIR) and the Department of Science and Technology (DST), Government of India.

References and Notes

(1) Laughlin, R. G. *The Aqueous Phase Behavior of Surfactants*; Academic Press: New York, 1994.

(2) Dickinson, E.; Euston, S. R.; Woskett, C. M. *Prog. Colloid Polym. Sci.* **1990**, *82*, 65.

(3) *Interfacial Phenomena in Petroleum Recovery*; Morrow, N. M., Ed.; Dekker: New York, 1991.
(4) Schwartz, L. J.; DeCiantis, C. L.; Chapman, S.; Kelley, B. K.; Hornak, J. P. *Langmuir* **1999**, *15*, 5461.
(5) Gragson, D. E.; McCarty, B. M.; Richmond, G. L. *J. Phys. Chem.* **1996**, *100*, 14272.
(6) Conboy, J. C.; Messmer, M. C.; Richmond, G. L. *J. Phys. Chem. B* **1997**, *101*, 6724.
(7) Conboy, J. C.; Messmer, M. C.; Richmond, G. L. *Langmuir* **1998**, *14*, 6722.
(8) Zhang, Z. H.; Tsuyumoto I.; Kitamori, T.; Sawada, T. *J. Phys. Chem. B* **1998**, *102*, 10284.
(9) Piasecki, D. A.; Wirth, M. J. *J. Phys. Chem.* **1993**, *97*, 7700.
(10) Tian, Y.; Umemura, J.; Takenaka, T.; Kunitake, T. *Langmuir* **1988**, *4*, 1064.
(11) Kjellin, U. R. M.; Claesson, P. M.; Linse, P. *Langmuir* **2002**, *18*, 6745.
(12) Lu, J. R.; Li, Z. X.; Thomas, R. K.; Staples, E. J.; Thompson, L.; Tucker, I.; Penfold, J. *J. Phys. Chem.* **1994**, *98*, 6559.
(13) Lu, J. R.; Su, T. J.; Li, Z. X.; Thomas, R. K.; Staples, E. J.; Tucker, I.; Penfold, J. *J. Phys. Chem. B* **1997**, *101*, 10332.
(14) Penfold, J.; Staples, E. J.; Tucker, I.; Thomas, R. K. *J. Colloid Interface Sci.* **1998**, *201*, 223.
(15) Lu, J. R.; Li, Z. X.; Thomas, R. K.; Binks, B. P.; Crichton, D.; Fletcher, P. D. I.; McNab, J. R.; Penfold, J. *J. Phys. Chem. B* **1998**, *102*, 5785.
(16) Penfold, J.; Thomas, R. K. *Phys. Chem. Chem. Phys.* **2002**, *4*, 2648.
(17) Penfold, J.; Tucker, I.; Staples, E.; Thomas, R. K. *Langmuir* **2004**, *20*, 7177.
(18) Tarek, M.; Tobias, D. J.; Klein, M. L. *J. Phys. Chem.* **1995**, *99*, 1393.
(19) Wijmans, C. M.; Linse, P. *J. Phys. Chem.* **1996**, *100*, 12583.
(20) Kuhn, H.; Rehage, H. *J. Phys. Chem. B* **1999**, *103*, 8493.
(21) Kuhn, H.; Rehage, H. *Phys. Chem. Chem. Phys.* **2000**, *2*, 1023.
(22) Kuhn, H.; Rehage, H. *Colloid Polym. Sci.* **2000**, *278*, 114.
(23) Dominguez, H. *J. Phys. Chem. B* **2002**, *106*, 5915.
(24) Stone, M. T.; da Rocha, S. R. P.; Rossky, P. J.; Johnston, K. P. *J. Phys. Chem. B* **2003**, *107*, 10185.
(25) Rekvig, L.; Hafskjold, B.; Smit, B. *J. Chem. Phys.* **2004**, *120*, 4897.
(26) Rekvig, L.; Hafskjold, B.; Smit, B. *Phys. Rev. Lett.* **2004**, *92*, 116101.
(27) Bandyopadhyay, S.; Chanda, J. *Langmuir* **2003**, *19*, 10443.
(28) Chanda, J.; Chakraborty, S.; Bandyopadhyay, S. *J. Phys. Chem. B* **2005**, *109*, 471.
(29) Chanda, J.; Bandyopadhyay, S. *J. Chem. Theory Comput.* **2005**, *1*, 963.
(30) Lu, J. R.; Li, Z. X.; Su, T. J.; Thomas, R. K.; Penfold, J. *Langmuir* **1993**, *9*, 2408.
(31) Martyna, G. J.; Tuckerman, M. E.; Tobias, D. J.; Klein, M. L. *Mol. Phys.* **1996**, *87*, 1117.
(32) Tuckerman, M. E.; Yarne, D. A.; Samuelson, S. O.; Hughs, A. L.; Martyna, G. J. *Comput. Phys. Commun.* **2000**, *128*, 333.
(33) Darden, T.; York, D.; Pedersen, L. *J. Chem. Phys.* **1993**, *98*, 10089.
(34) Procacci, P.; Darden, T.; Marchi, M. *J. Phys. Chem.* **1996**, *100*, 10464.
(35) Procacci, P.; Marchi, M.; Martyna, G. J. *J. Chem. Phys.* **1998**, *108*, 8799.
(36) Allen, M. P.; Tildesley, D. J. *Computer Simulation of Liquids*; Clarendon: Oxford, UK, 1987.
(37) Berendsen, H. J. C.; Grigera, J. R.; Straatsma, T. P. *J. Phys. Chem.* **1987**, *91*, 6269.
(38) Martin, M. G.; Siepmann, J. I. *J. Phys. Chem. B* **1998**, *102*, 2569.
(39) Jorgensen, W. L. *J. Phys. Chem.* **1986**, *90*, 1276.
(40) Briggs, J. M.; Matsui, T.; Jorgensen, W. L. *J. Comput. Chem.* **1990**, *11*, 958.
(41) Tu, K.; Tobias, D. J.; Blasie, J. K.; Klein, M. L. *Biophys. J.* **1996**,*70*, 595.
(42) Rao, M.; Berne, B. J. *Mol. Phys.* **1979**, *37*, 455.
(43) Hill, T. L. *Introduction to Statistical Mechanics*; Dover: New York, 1986.
(44) Jang, S. S.; Lin, S. T.; Maiti, P. K.; Blanco, M.; Goddard, W. A., III; Shuler, P.; Tang, Y. *J. Phys. Chem. B* **2004**, *108*, 12130.
(45) Liu, P.; Harder, E.; Berne, B. J. *J. Phys. Chem. B* **2004**, *108*, 6595.
(46) Christensen, M.; Pedersen, J. B. *J. Chem. Phys.* **2003**, *119*, 5171.
(47) Balasubramanian, S.; Bagchi, B. *J. Phys. Chem. B* **2002**, *106*, 3668.
(48) Pal, S.; Bagchi, B.; Balasubramanian, S. *J. Phys. Chem. B* **2005**, *109*, 12879.
(49) Faeder, J.; Ladanyi, B. M. *J. Phys. Chem. B* **2000**, *104*, 1033.